Increase in short-chain ceramides correlates with an altered lipid organization and decreased barrier function in atopic eczema patients

Michelle Janssens,[1,*] Jeroen van Smeden,[1,*] Gert S. Gooris,[*] Wim Bras,[†] Guiseppe Portale,[†] Peter J. Caspers,[§,] Rob J. Vreeken,[††,§§] Thomas Hankemeier,[††,§§] Sanja Kezic,[***] Ron Wolterbeek,[†††] Adriana P. Lavrijsen,[§§§] and Joke A. Bouwstra[2,*]**

Department of Drug Delivery Technology,* Department of Analytical Biosciences,[††] and Netherlands Metabolomics Centre,[§§] Leiden/Amsterdam Center for Drug Research, Leiden University, Leiden, The Netherlands. Netherlands Organization for Scientific Research,[†] Dutch Belgian Beamline Collaborating Research Group / European Synchrotron Radiation Facility, Grenoble, France. Center for Optical Diagnostics and Therapy,[§] Department of Dermatology, Erasmus MC, Rotterdam, The Netherlands. River Diagnostics BV,** Rotterdam, The Netherlands. Coronel Institute of Occupational Health,*** Academic Medical Center, University of Amsterdam, Amsterdam, The Netherlands. Department of Medical Statistics and Bioinformatics[†††] and Department of Dermatology,[§§§] Leiden University Medical Center, Leiden, The Netherlands

Abstract A hallmark of atopic eczema (AE) is skin barrier dysfunction. Lipids in the stratum corneum (SC), primarily ceramides, fatty acids, and cholesterol, are crucial for the barrier function, but their role in relation to AE is indistinct. Filaggrin is an epithelial barrier protein with a central role in the pathogenesis of AE. Nevertheless, the precise causes of AE-associated barrier dysfunction are largely unknown. In this study, a comprehensive analysis of ceramide composition and lipid organization in nonlesional SC of AE patients and control subjects was performed by means of mass spectrometry, infrared spectroscopy, and X-ray diffraction. In addition, the skin barrier and clinical state of the disease were examined. The level of ceramides with an extreme short chain length is drastically increased in SC of AE patients, which leads to an aberrant lipid organization and a decreased skin barrier function. Changes in SC lipid properties correlate with disease severity but are independent of filaggrin mutations. We demonstrate for the first time that changes in ceramide chain length and lipid organization are directly correlated with the skin barrier defects in nonlesional skin of AE patients. We envisage that these insights will provide a new therapeutic entry in therapy and prevention of AE.—Janssens, M., J. van Smeden, G. S. Gooris, W. Bras, G. Portale, P. J. Caspers, R. J. Vreeken, T. Hankemeier, S. Kezic, R. Wolterbeek, A. P. Lavrijsen, and J. A. Bouwstra. **Increase in short-chain ceramides correlates with an altered lipid organization and decreased barrier function in atopic eczema patients. *J. Lipid Res.* 2012.** 53: **2755–2766.**

Supplementary key words ceramide composition • lamellar phase • lateral packing

The skin offers a protective barrier against allergens, irritants, and microorganisms and prevents excessive transepidermal water loss (TEWL). The barrier function strongly relies on the outermost layer of the skin, the stratum corneum (SC), which consists of corneocytes embedded in a highly organized lipid matrix (1, 2). This lipid matrix is considered to be important for a proper skin barrier function.

Ceramides (CER), cholesterol, and free fatty acids are the main lipid classes in SC. To date, 12 CER subclasses in human SC have been identified with a wide chain length distribution (3, 4). An explanation of the CER nomenclature is given in **Fig. 1**. The aim of the present study was to determine the chain lengths of each CER subclass in nonlesional skin of atopic eczema (AE) patients and to correlate these with lipid organization, skin barrier function, and disease severity (**Fig. 2**).

AE is a chronic relapsing inflammatory skin disease characterized by a broad spectrum of clinical manifestations, such as erythema, dryness, and intense pruritus (5, 6). AE affects over 15% of Caucasian children and 2–10% of adults, and its prevalence is increasing rapidly, especially in developed countries (7–11). Patients have a decreased

This work was supported by European Cooperation in Science and Technology (COST) and by Stichting Technische Wetenschappen (STW) Grant 10064. At the time of this study, P.J.C. was an employee of River Diagnostics B.V.

Manuscript received 11 July 2012 and in revised form 25 September 2012.

Published, JLR Papers in Press, September 28, 2012
DOI 10.1194/jlr.P030338

Abbreviations: AE, atopic eczema; CER, ceramide; FLG, filaggrin; FTIR, Fourier transform infrared spectroscopy; LPP, long periodicity phase; NMF, natural moisturizing factor; SAXD, small angle X-ray diffraction; SC, stratum corneum; SCORAD, scoring atopic dermatitis; SPP, short periodicity phase; TEWL, transepidermal water loss.

[1] M. Janssens and J. van Smeden contributed equally to this work.
[2] To whom correspondence should be addressed.
e-mail: Bouwstra@chem.leidenuniv.nl

The online version of this article (available at http://www.jlr.org) contains supplementary data in the form of five figures and five tables.

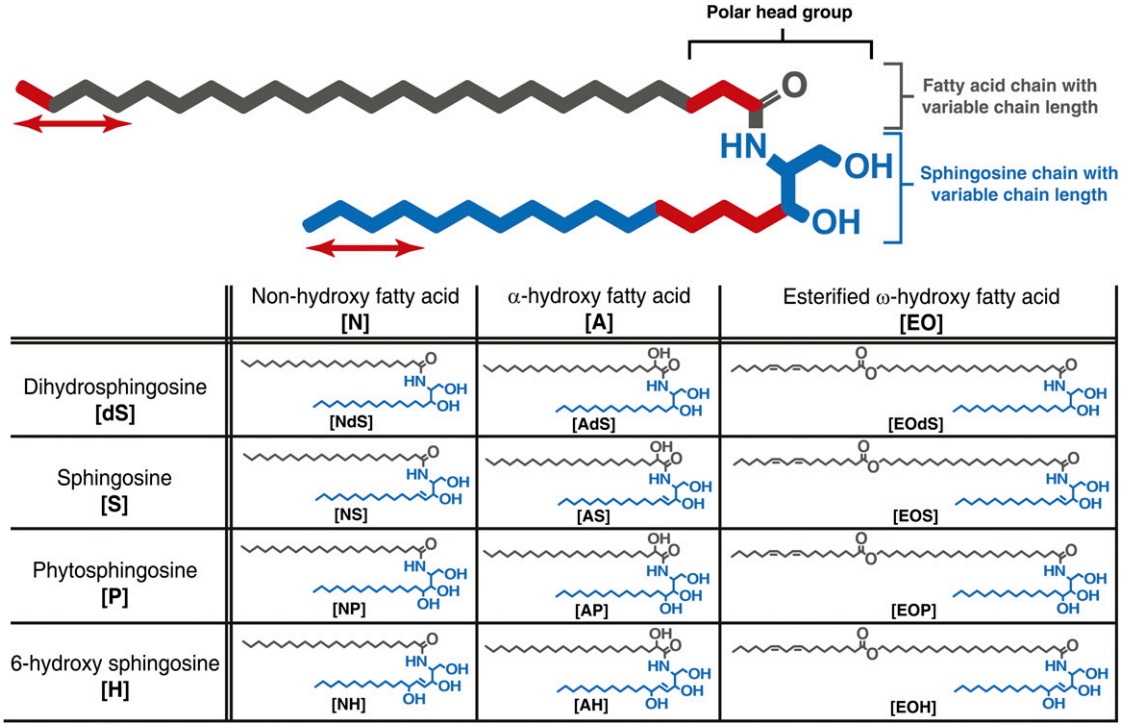

Fig. 1. Structure and nomenclature of CERs. All CERs bear a polar head group and two long carbon chains. The polar head group may vary in molecular architecture (at the carbon positions marked in red), resulting in 12 different subclasses in human SC. Both chains in every CER subclass show varying carbon chain lengths (marked by red arrows). Each CER subclass is denoted by its sphingoid base (blue) and fatty acid chain (gray), resulting in the 12 CER subclasses. Sphingoid base abbreviations: dS, dihydrosphingosine; H, 6-hydroxy sphingosine; P, phytosphingosine; S, sphingosine. Acyl chain abbreviations: A, α-hydroxy fatty acid; EO, esterified ω-hydroxy fatty acid; N, non-hydroxy fatty acid. These abbreviations result in the 12 CER subclasses notations: [NdS], [AdS], [EOdS], [NS], [AS], [EOS], [NP], [AP], [EOP], [NH], [AH], [EOH]. The number of total carbon atoms in the CERs (e.g., C34 CERs) is the number of carbon atoms in the fatty acid chain plus the number of carbon atoms in the sphingoid base.

skin barrier function in lesional and nonlesional skin (12–16).

In previous studies, it has been shown that AE is strongly associated with mutations in the filaggrin gene (*FLG*) (17–19), but the role of *FLG* mutations for the barrier dysfunction is yet inconclusive (20–25). Other factors, such as aberrations in the SC lipids, may play a role in the decreased skin barrier in AE (12, 26, 27). In healthy SC, lipids form two lamellar phases with repeat distances of approximately 6 and 13 nm. These are referred to as the short periodicity phase (SPP) and long periodicity phase (LPP), respectively (28, 29). A schematic presentation of the lipid organization is provided in **Fig. 3**. Within the lipid lamellae, the lipids have a dense (orthorhombic) lateral organization, although a subpopulation of the lipids can be less densely packed in a hexagonal organization (30–32).

CERs play a crucial role in the lipid organization (33), and they have a characteristic molecular architecture. Several studies have reported significant changes in CER subclasses in nonlesional SC of AE patients: reduced CER [NP], increased CER [AS], and reduced long chain CERs [EOH] and [EOS] (12, 23, 34–36). Some of these changes could be correlated with changes in skin barrier function. However, no information was reported on the effect of chain length distribution of CERs on the skin barrier until recently. Ishikawa et al. showed that lesional skin has a significantly increased level of short-chain CERs (with a total chain length of 34 carbon atoms) in one specific CER subclass, which correlates with the impaired skin barrier function (37). These results suggest that CER chain length may be an important factor in skin barrier dysfunction of AE patients. These findings were the starting point of the present study, in which we performed a detailed analysis on CER composition, focusing in particular on the CER chain length distribution in nonlesional SC of AE patients in relation to lipid organization and skin barrier dysfunction. We studied SC of nonlesional skin, as we aimed to monitor the changes in lipid properties in the

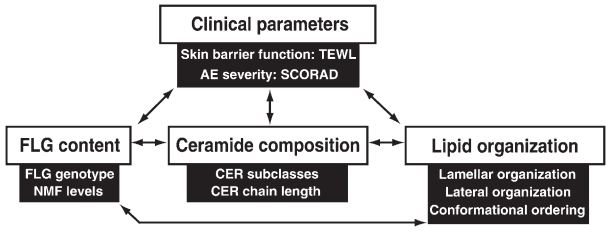

Fig. 2. Schematic overview of the SC lipid parameters, clinical parameters, and the determinants of the filaggrin content discussed in this article. These parameters may all affect the skin barrier and are therefore investigated in this study. Arrows indicate possible correlations that are discussed.

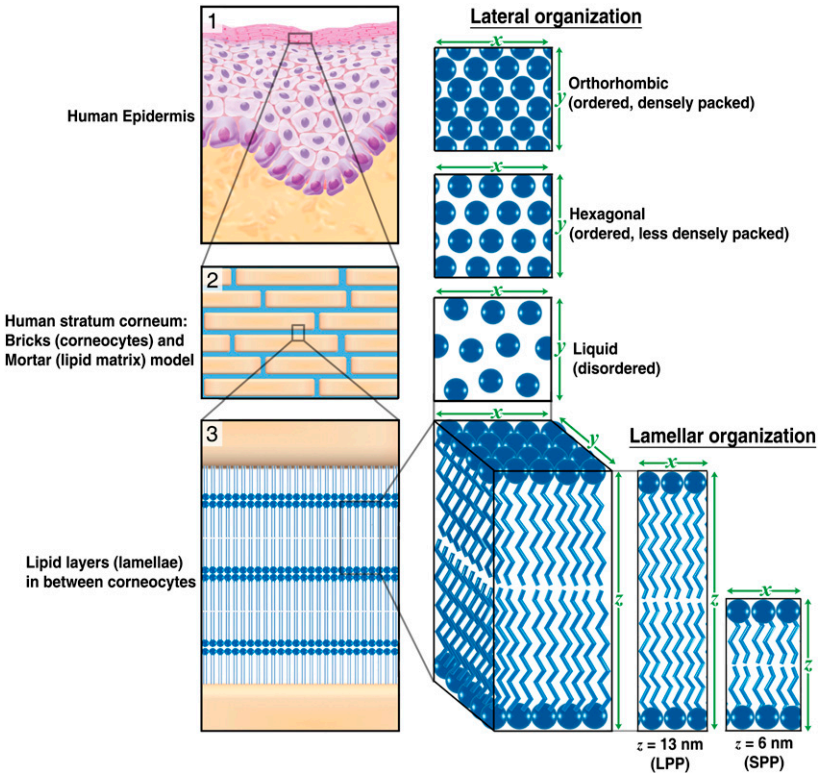

Fig. 3. Lamellar and lateral organization in human stratum corneum. (1) The outermost layer of the epidermis, the SC, consists of dead cells (corneocytes) embedded in a lipid matrix, also referred to as the brick (corneocytes) and mortar (lipids) structure (2). The intercellular lipids are arranged in layers (lamellae) (3), with two coexisting lamellar phases. These lamellar phases have a repeat distance of 6 nm (referred to as the SPP) or 13 nm (referred to as the LPP). The lateral organization is the plane perpendicular to the direction of the lamellar organization. There are three possible arrangements of the lipids: a very dense, ordered orthorhombic organization; a less dense, ordered hexagonal organization; and a disordered liquid organization.

absence of inflammation. We have identified several CER subclasses that exhibit an increased level of extremely short C34 chains in AE, and we demonstrate that the overall level of C34 is increased in AE. The changes in CER chain length distribution correlated with changes in lipid organization, skin barrier function, disease severity, and levels of natural moisturizing factor (NMF, composed of filaggrin-derived amino acids, their metabolites, specific sugars, and salts). Changes in CER chain length distribution did not correlate with *FLG* genotype. These results demonstrate for the first time that CER chain length is an important factor in skin barrier dysfunction in nonlesional skin of AE.

MATERIAL AND METHODS

Study population and general study setup

The study was conducted in accordance with the Declaration of Helsinki and was approved by the Ethical Committee of the Leiden University Medical Center. All subjects gave written informed consent. Fifteen Caucasian subjects without (history of) dermatological disorders (25.0 ± 5.2 years; 5 males) and 28 Caucasian AE patients (25.6 ± 5.6 years; 11 males) were included. The group of AE patients consists of 14 patients with and 14 patients without the presence of common *FLG* genotype mutations (see *FLG* mutation analysis below). Subjects did not apply any dermatological products to their forearms for at least one week prior to the study. The study itself was performed in a temperature- and humidity-controlled room, and subjects were acclimatized for 45 min prior to the measurements. Per subject, all measurements were performed on a single day on one of the ventral forearms, which was observed by a dermatologist at the start of the study to carefully depict an area of nonlesional skin, which was marked accordingly. At this area, NMF levels were determined with Raman spectroscopy, followed by subsequent tape stripping, TEWL, and Fourier transform infrared spectroscopy (FTIR) measurements, as described below. At the end of the study day, buccal mucosa cells were collected with a cotton swab, and scoring atopic dermatitis (SCORAD) was performed by a dermatologist to determine the severity of the disease. Finally, a 4 mm biopsy was harvested close to the area where all measurements were performed.

FLG mutation analysis

The influence of *FLG* mutations on lipid properties was studied. We screened all subjects on the four most prevalent mutations found in European Caucasians (2282del4, R501×, S3247×, and R2447×), covering around 93% of all *FLG* mutations known to date (38). Buccal mucosa cells were collected by rubbing the inside of the cheeks with a cotton swab on a plastic stick after rinsing the mouth with water. Mutations were determined by genotyping after DNA extraction (39).

Skin barrier function assessment by TEWL

A Tewameter TM 210 (Courage+Khazaka, Köln, Germany) was used to measure TEWL on the marked area on the ventral forearm of the subject. The forearm was placed in an open chamber, and TEWL values were recorded for 2 min, after which an average reading during the last 10 s of the measurement was calculated. This procedure was performed before tape stripping (baseline TEWL) and after every two tape strips to have an indication of the amount of removed SC.

SCORAD

SCORAD was performed by the dermatologist to determine the severity of the disease (40).

Determination of NMF levels in SC

Confocal Raman microspectroscopy (3510 Skin Composition Analyzer, River Diagnostics, Rotterdam, The Netherlands) was used to measure NMF in the SC of the ventral forearm. The principles and experimental details of this method and the procedure have been described elsewhere (41, 42). Depth profiles of Raman spectra were measured at 2 μm intervals from the skin surface to 20 μm below the skin surface. In each subject, 15 profiles were measured at different spots within the marked area on the ventral forearm. Raman spectra were recorded between 400 and 1,800 cm^{-1} with a 785 nm laser. Laser power on the skin was 25 mW. NMF levels relative to keratin were determined from the Raman spectra measured between 4 and 8 μm by means of classical least-squares fitting. Relative NMF to keratin levels were calculated from the recorded Raman spectra by using SkinTools 2.0 (River Diagnostics).

Tape stripping procedure

To harvest SC lipids, the following tape stripping procedure was performed on both control subjects and nonlesional regions of AE patients: multiple poly(phenylene sulfide) tape strips (Nichiban, Tokyo, Japan) were successively applied at the same area (4.5 cm^2) on the ventral forearm. All tapes were pressed to the targeted skin with a pressure of 450 g/cm^2 using a D-Squame pressure instrument (Cuderm Corp., Dallas, TX). Tweezers were used to remove the tape in a fluent stroke, using alternating directions for each successive tape strip. The Squamescan 850A (Heiland Electronic, Wetzlar, Germany) was used to determine the amount of SC removed to obtain a good indication of the depth of each tape strip taken (43, 44). Calibration was performed by a bicinchoninic acid (BCA) assay using BSA. The predicted total amount of protein in the SC was calculated by plotting 1/TEWL against the cumulative amount of protein removed. The intercept with the *x* axis is indicative for the total amount of protein in the SC according to Kalia (43). Tapes 6–9 were selected for lipid composition analysis, as these tapes do not show surface contamination (observed when analyzing tape strips from the surface of the SC). All tapes were punched to a circular area of 2 cm^2, put individually into glass vials containing 1 ml chloroform/methanol/water (1:2:1/2) and stored at −20°C under argon atmosphere prior to lipid extraction.

Lipid extraction and ceramide analysis by LC/MS

Lipid extraction was performed on four tape strips (numbers 6–9) of each subject. Before lipids were extracted from tape strips by liquid-liquid extraction, two deuterated internal ceramide standards (CER [NS] C24 and, CER [EOS] C30 linoleate) were added to compare CER levels between control group and nonlesional skin of AE patients. Then, a slightly enhanced extraction procedure of the commonly used Bligh and Dyer method was performed on all four selected tape strips individually: three different ratios of solvent mixtures chloroform/methanol/water (1:2:1/2; 1:1:0; 2:1:0) were used sequentially to extract all lipids. A detailed procedure is described elsewhere (45, 46). Afterwards, lipid extracts from all four individual tapes were pooled, dried under N_2 gas, and resolved in 100 μl chloroform/methanol/heptane (2.5:2.5:95) to obtain a total lipid concentration around 1.0 mg/ml. Samples were stored at −20°C until use. The analysis was performed by LC/MS using a recently developed LC/MS method described in detail elsewhere (4). Briefly, 10 μl of each lipid sample was automatically injected and separated onto an analytical normal phase column [PVA-bonded column; 100 × 2.1 mm id, 5 μm particle size, YMC (Kyoto, Japan)] by a gradient solvent system from heptane to heptane/IPA/ethanol at a flow rate of 0.8 ml/min using an Alliance 2695 HPLC system (Waters, Milford, MA). The HPLC was coupled to a mass spectrometer (TSQ Quantum, Thermo Finnigan, San Jose, CA) in APCI-positive mode with a scan range set at 360–1200 amu. The temperature of the source heater and heated capillary were set to 450°C and 250°C, respectively, and the discharge current was set to 5 μA. The ceramide analysis was performed using Xcalibur software version 2.0, and its nomenclature used throughout this article is according to Motta (47), in which ceramide subclasses are classified by letter abbreviations according to their two individual chains: the sphingoid base [either dihydrosphingosine (dS), sphingosine (S), 6-hydroxy sphingosine (H) or phyto-sphingosine (P)] chemically linked to the fatty acid chain [either an α-hydroxy fatty acid (A), an esterified ω-hydroxy fatty acid (EO), or a non-hydroxy fatty acid (N)]. This results in 12 different CER subclasses, namely, [AdS], [AS], [AH], [AP], [EOdS], [EOS], [EOH], [EOP], [NdS], [NS], [NH], and [NP]. The CER nomenclature and its molecular structure are explained in Fig. 1.

Lateral organization and conformational ordering of the lipids

To obtain information on the lateral organization and conformational ordering of the lipids, FTIR spectra were recorded in the same skin region also used for lipid analysis. FTIR spectra of the SC were collected after each two tape strips using a Varian 670-IR spectrometer (Varian Inc., Santa Clara, CA) equipped with a broad band Mercury-Cadmium-Telluride (MCT) detector and an external sample compartment containing a Gladi-*ATR* (Pike, Madison, WI) attenuated total reflection (ATR) accessory with a single-reflection diamond. The spectral resolution was 2 cm^{-1}. The instrument was continuously purged with dry N_2. Each spectrum was an average of 150 scans. For data treatment, the instrument software Resolutions Pro 4.1 (Varian Inc.) was used. We calculated positions of the CH_2 symmetric stretching vibration and second derivatives of the scissoring bandwidth as described previously (48, 49). Shortly, the second derivative was calculated, and it was baseline corrected between the endpoints of the scissoring region (∼1,460–1,480 cm^{-1}). We calculated the bandwidth at 50% of the peak height (full width half maximum, FWHM) and determined CH_2 symmetric stretching vibration positions of spectra recorded between the removal of 2–10 tape strips.

Biopsy and small angle X-ray diffraction measurements

After tape stripping, 4 mm biopsies were taken from the ventral forearm close to the region of the tape stripping. SC was isolated by trypsin digestion as described earlier (50). This procedure does not affect the lipid organization in SC (51). The SC sheets were measured by small angle X-ray diffraction (SAXD) performed at the European Synchrotron Radiation Facility (ESRF, Grenoble, France) using station BM26B. Prior to the measurements, SC was hydrated over a 27% NaBr solution

during 24 h. To obtain high-quality diffraction patterns, SC was carefully oriented parallel to the primary X-ray beam. SAXD patterns were detected with a Frelon 2000 CCD detector at room temperature for a period of 10 min using a microfocus beam, similarly as described elsewhere (52). Samples were checked for evidence of radiation damage, and exposure time to X-rays was kept to a minimum. From the scattering angle, the scattering vector (q) was calculated by $q = 4\pi \sin \theta/\lambda$, in which λ is the wavelength of the X-rays at the sample position and θ the scattering angle.

Statistical analysis

Statistical analysis was performed using SPSS Statistics. Nonparametric Mann-Whitney tests were performed when comparing two groups and stated significant when $P < 0.05$. When the effect of *FLG* was taken into account and trends were observed, Kruskall-Wallis tests and, eventually, an additional Mann-Whitney test was performed. Bivariate analysis was performed to analyze which parameters showed a significant correlation, and their respective Spearman's ρ correlation coefficients were calculated. Univariate general linear model analysis was performed to correlate the biologically and clinically relevant parameters to two independent lipid parameters, as well as to the predicted and the observed average chain length.

RESULTS

Description of study population

Fourteen out of 28 AE patients were carriers of at least one of the four most common *FLG* mutations (details in supplementary Table I). Patient and control subject characteristics are provided in supplementary Table II. Two control subjects were heterozygous for *FLG* mutations. Severity of the disease was scored by an experienced dermatologist using SCORAD (**Fig. 4A**). AE patients showed an elevated TEWL in nonlesional skin compared with control subjects (12.2 ± 6.5 g/m^2/h and 6.5 ± 1.7 g/m^2/h, respectively; $P < 0.0005$) (Fig. 4B) and lower NMF levels compared with control subjects (0.66 ± 0.39 and 1.05 ± 0.20, respectively; $P < 0.01$) (Fig. 4C).

Reduced CER chain length correlates with a decreased barrier function

From the LC/MS data, lipid profiles were constructed, and examples are shown in supplementary Fig. I. From manual integration of these lipid profiles, the relative abundance of all CER subclasses could be calculated (supplementary Fig. II). Statistical differences between control subjects and AE patients were observed in seven subclasses: CERs [EOP], [EOH], [NS], [NP], [NH], [AS], and [AH] ($P < 0.05$). No difference was observed between carriers and noncarriers of *FLG* mutations. The total CER level in the control group and in nonlesional skin of AE patients was not significantly different (37.0 ± 3.6 and 38.5.4 ± 2.4 ng/μg protein, respectively; $P > 0.1$).

The average CER chain length was significantly decreased by 0.64 ± 0.23 total carbon atoms in AE patients (mean ± SEM; $P = 0.012$) (**Fig. 5A**). No difference was observed between carriers and noncarriers of *FLG* mutations ($P > 0.1$). Fig. 5A shows that in nonlesional skin of AE patients, extremely short C34 CERs were increased within several CER subclasses. This was primarily observed in CER subclasses [AS], [AH], [NS], and [NH] ($P < 0.05$) (Fig. 5B). The increase in total C34 CERs in AE ($P < 0.0001$) contributes to a reduction in overall chain length. In addition, the very long chain CERs belonging to the [EO] subclass are significantly reduced, which is primarily caused by significantly decreased levels of CER [EOH] and [EOP] ($P = 0.019$ and $P = 0.040$, respectively) (Fig. 5A and supplementary Fig. II-B). Univariate analysis shows that an increased level of C34 CERs and decreased level of CERs [EO] largely contribute to a reduction in average CER chain length, as can be observed from Fig. 5C. The influence of *FLG* mutations on any of the CER chain length parameters was not significant ($P > 0.1$) (detailed overview in supplementary Tables III–V).

The observed changes in CER chain length were compared with changes in barrier function as assessed by TEWL. The results in Fig. 5D show a strong correlation

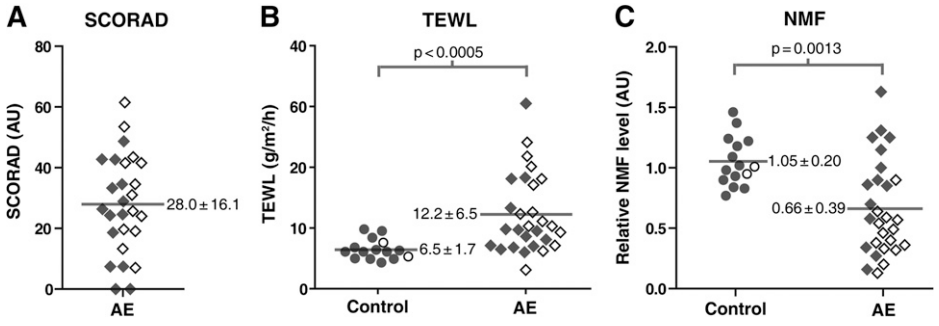

Fig. 4. SCORAD, TEWL, and NMF levels in control subjects and AE patients. Dot plots showing individual control subjects (open and filled circles) and AE patients (open and filled diamonds) of the measured parameters (A) SCORAD, (B) TEWL, and (C) NMF levels. Open and filled data points indicate carriers and noncarriers of *FLG* mutations, respectively. Means are indicated by gray horizontal lines and their corresponding values (± SD). Significant differences were observed between control subjects and AE patients for both TEWL and NMF. *FLG* mutations were associated with reduced NMF levels in AE patients ($P < 0.005$) but not with SCORAD and TEWL.

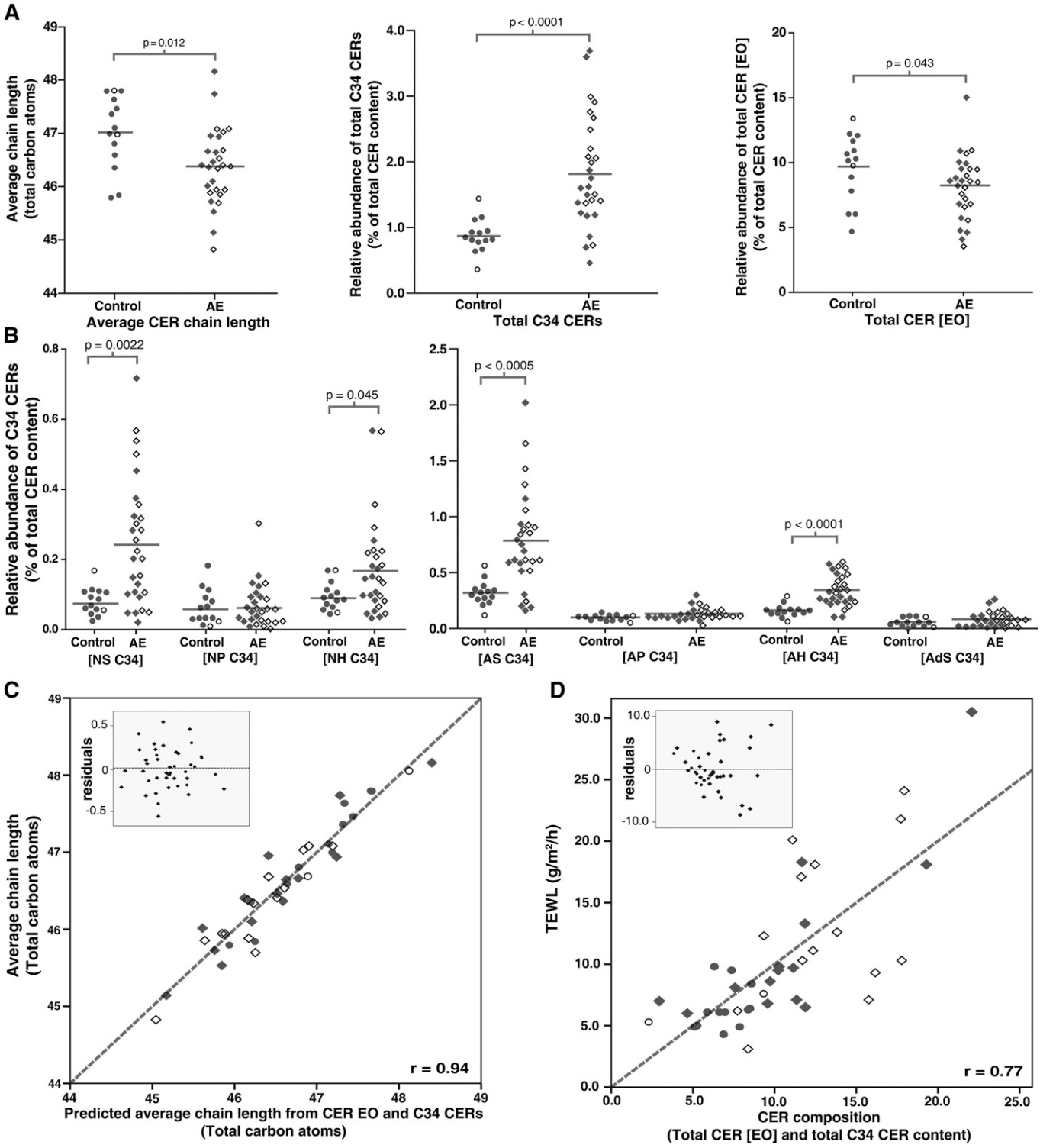

Fig. 5. CER composition in control subjects and AE patients. (A) Dot plot showing the average chain length of all CERs in total; the relative abundance of total C34 CERs, and the relative abundance of total [EO] CERs. (B) Dot plots indicating the relative abundance of C34 CER species for each subclass. (C) Scatter plot of univariate analysis of the predicted average chain length (by the abundance of C34 CERs and [EO] CERs) versus the observed average chain length. Gray dotted line represents the optimal fit ($r = 0.94$): Average chain length = $(0.33 \times \text{C34 CERs}) + (0.24 \times \text{CER[EO]})$. (D) Scatter plot of univariate analysis of C34 CER and CER [EO] versus the TEWL. Insets show the residuals of the respective plots. Gray dotted line represents the optimal fit ($r = 0.77$): TEWL = $8.2 + (4.6 \times \text{C34 CERs}) - (0.6 \times \text{CER[EO]})$. Control subjects are indicated by open and filled circles. AE patients with are indicated by open and filled diamonds. Data points indicate carriers and noncarriers of *FLG* mutations, respectively.

between TEWL and the levels of C34 CERs and CER [EO]: univariate analysis of TEWL versus the total C34 CERs and total CER [EO] levels shows a correlation coefficient of 0.77 ($P < 0.0001$).

Correlations between the relative abundances of the various CER subclasses with TEWL are shown in **Table 1**. CER [EOH] and CER [AS] are the two subclasses that are most significantly associated with TEWL. This again indicates the importance of the chain length for the skin barrier in AE: the exceptionally long CER [EOH] is decreased, whereas CER [AS], the CER subclass with the highest abundance of exceptionally short C34 CERs, is increased. The changes in CER composition are irrespective of *FLG* mutation status ($P = 0.58$).

Altered lamellar and lateral lipid organization correlates with a decreased barrier function

SAXD gives information about the lamellar organization of intercellular lipids in SC (28) (explanation in supplementary Fig. III). The lipids form two lamellar phases, the SPP and LPP. **Fig. 6A** shows three examples of SAXD curves of SC. The upper curve is a typical example from a control subject. The central curve is typical for AE. The bottom curve is representative for a subgroup of AE patients with an aberrant SAXD profile. The upper two curves show lipid-based features as two weak diffraction peaks (labeled I and III) and a strong peak (labeled II). The LPP contributes to all three peaks, whereas the SPP contributes only to peak II (supplementary Fig. III). In the bottom curve, both peaks I and III are absent, and peak II is shifted to higher q-values. Peaks I and III were not present in 5 out of 28 patients. As peak I and peak III are attributed only to the LPP, this indicates that there is a drastic reduction in the presence of the LPP in those patients.

Fig. 6B shows the position of the strong peak (II) in the SAXD curves from control subjects (left) and AE patients (right). The peak position shows a larger variance within the group of AE patients compared with the group of control subjects. The average position of the strong peak is located at significantly higher q-values for AE patients compared with control subjects (1.03 nm^{-1} and 1.00 nm^{-1}, respectively; $P = 0.046$). The position of peak II showed no difference between AE patients with and patients without *FLG* mutations ($P = 0.76$).

FTIR was used to obtain information on the lateral lipid organization. Two types of vibrations were monitored, the CH_2 symmetric stretching vibrations and the CH_2 scissoring vibrations (supplementary Fig. IV). A low (~2,848 cm^{-1}) wave number of the CH_2 symmetric stretching vibrations indicates the presence of a highly ordered lipid organization (either hexagonal or orthorhombic), whereas a high (2,853 cm^{-1}) wave number indicates a liquid disordered phase (53). The mean value of the position of the CH_2 symmetric stretching vibrations of AE patients shows a small but significant shift to higher values compared with control subjects (2,849.2 cm^{-1} versus 2,848.8 cm^{-1}, respectively; $P = 0.0013$) (Fig. 6C). In addition, the variance in the group of AE patients is larger than in control subjects. To distinguish between an orthorhombic (dense) or hexagonal (less dense) lateral organization, the bandwidth of the CH_2 scissoring vibrations was monitored. A narrow bandwidth (typically 8 cm^{-1}) indicates the presence of only a hexagonal lipid organization, whereas a large bandwidth of typically 11 cm^{-1} is indicative for the presence of mainly an orthorhombic organization (49). The average bandwidth of the scissoring vibrations was significantly lower in AE patients compared with control subjects (10.6 cm^{-1} versus 11.6 cm^{-1}, respectively; $P = 0.010$) (Fig. 6D), demonstrating a reduction of lipids in an orthorhombic organization and thus a less dense lipid organization. No significant influence of *FLG* mutations on the lipid organization in AE patients was found ($P > 0.05$) (Fig. 6B–D).

Univariate analysis was performed between TEWL and two independent lipid organization parameters: a lamellar organization component (SAXD peak II position) and a lateral organization component (FTIR scissoring bandwidth). The correlation coefficient was $r = 0.76$ ($P < 0.0001$) (Fig. 6E), which demonstrates that skin barrier function as measured by TEWL is significantly influenced by lipid organization.

TABLE 1. Correlation coefficients of CER subclasses versus TEWL

CER Subclass	TEWL
CER [EOdS]	−0.245
CER [EOS]	−0.177
CER [EOP]	−0.434**
CER [EOH]	−0.617***
CER [NdS]	−0.226
CER [NS]	0.407**
CER [NP]	−0.483**
CER [NH]	−0.420**
CER [AdS]	0.214
CER [AS]	0.650***
CER [AP]	0.255
CER [AH]	0.195
Total CER [EO]	−0.441**
Total C34 CERs	0.738***
Average CER chain length	−0.528***

The table contains all 12 CER subclasses as well as the CER that strongly influence the chain length (i.e., total CER [EO] and total C34 CER).
**$P < 0.01$.
***$P < 0.001$.

Altered CER composition correlates with aberrant lipid organization

As CER composition and lipid organization both show a relationship with a reduced skin barrier (TEWL), the relation between the lipid parameters is summarized in **Table 2**. The levels of C34 CERs and CER [EO] associate with both the lamellar organization (SAXD) and lateral lipid organization (FTIR scissoring bandwidth and stretching vibrations position). A powerful correlation of 0.71 was observed when both the lamellar and lateral organization components (SAXD and CH_2 scissoring) were plotted versus the two components of the CER composition ([EO] CERs and C34 CERs). Supplementary Fig. V illustrates this correlation.

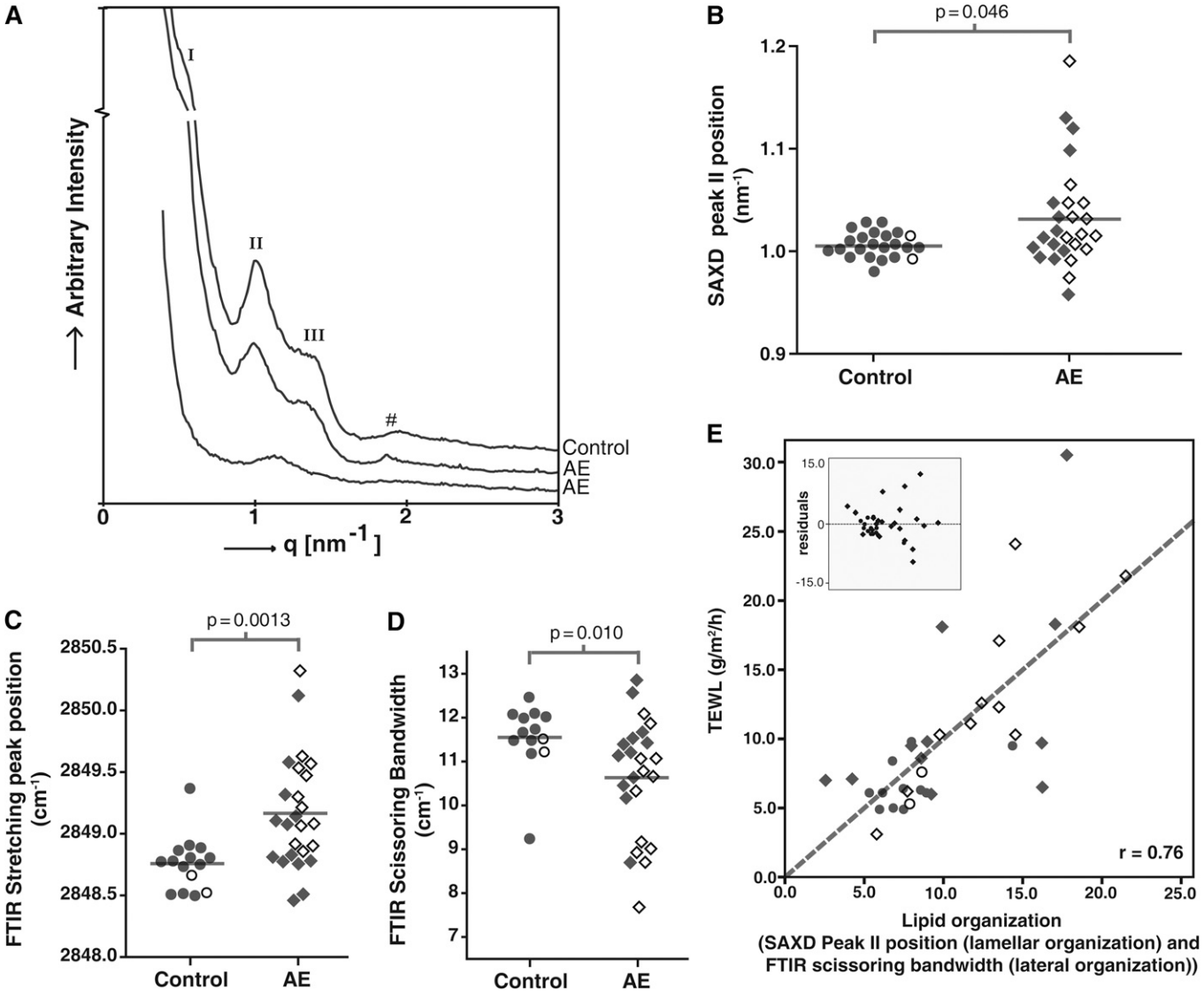

Fig. 6. Lipid organization in control subjects and AE patients. (A) The upper SAXD curve of a control subject shows the first (I), second (II), and third (III) order peak positions of the LPP. #Phase-separated cholesterol. The middle diffraction curve is from an AE patient and resembles the pattern of SC of the control subject. The bottom curve of an AE patient shows only the presence of peak II. (B) Position of peak II in SAXD curves. (C) Position of the stretching vibrations in the FTIR spectrum. (D) Scissoring bandwidth in the FTIR spectrum. (E) Correlation between lipid organization and TEWL. Scatter plot of univariate analysis of SAXD peak II position + bandwidth of scissoring vibrations versus the TEWL. The inset shows the residuals of this plot. The gray dotted line represents the optimal fit ($r = 0.76$): TEWL = $-30.1 + (64 \times$ SAXD peakII position$) - (2.3 \times$ Bandwidth). The correlation coefficient is 0.76. Control subjects are indicated by open and filled circles AE patients with are indicated by open and filled diamonds. Data points indicate carriers and noncarriers of *FLG* mutations, respectively.

Altered CER composition and aberrant lipid organization correlate with NMF levels and SCORAD

A detailed overview of correlation coefficients between different parameters is presented in **Table 3**. NMF levels correlate ($r > 0.4$; $P < 0.01$) with both lamellar and lateral lipid organization as well as with chain length of the CERs. SCORAD (disease severity) was associated with CER composition (i.e., total C34 CERs and total CER [EO] content) and lipid organization (i.e., SAXD peak II position and FTIR scissoring bandwidth), with correlation coefficients of 0.56 ($P < 0.01$) and 0.58 ($P < 0.01$), respectively.

FLG mutations correlate with NMF levels, but not with SCORAD and TEWL levels

NMF levels were significantly lower in *FLG* carriers than in noncarriers (0.45 ± 0.19 and 0.87 ± 0.43, respectively; $P < 0.005$). Both SCORAD and TEWL values were independent of *FLG* genotype ($P = 0.34$ and $P = 0.23$. respectively).

DISCUSSION

We performed an integral analysis of CER composition focusing on the chain length distribution of each of the CER subclasses in relation to lipid organization and their

TABLE 2. Correlation coefficients of lipid composition and lipid organization parameters

Lipid Organization / CER Composition Parameter	Correlation Coefficient (r)
SAXD peak II position versus total C34 CER content	0.432**
SAXD peak II position versus total CER [EO] content	−0.393**
SAXD peak II position versus average CER chain length	−0.370*
FTIR scissoring bandwidth versus total C34 CER content	−0.669***
FTIR scissoring bandwidth versus total CER [EO] content	0.267
FTIR scissoring bandwidth versus average CER chain length	0.386*
FTIR stretching versus total C34 CER content	0.607***
FTIR stretching versus total CER [EO] content	−0.399*
FTIR stretching versus average CER chain length	−0.471**

*$P < 0.05$.
**$P < 0.01$.
***$P < 0.001$.

correlation with skin barrier function (TEWL), disease severity (SCORAD), *FLG* mutations, and NMF levels. This study provides detailed information about the role of lipids in the impaired skin barrier function of nonlesional AE skin.

The results show a reduced average CER chain length in nonlesional skin of AE patients. This reduction in chain length can be attributed to an increase in extremely short C34 CERs as well as a reduction in very long CER [EO] subclasses. The increment in C34 CERs has recently been reported by Ishikawa et al. for a single subclass (CER [NS]) in lesional skin of AE patients (37). Here we show in nonlesional skin a largely increased level of C34 CERs in four CER subclasses: CER [NS], [NH], [AS], and [AH].

TABLE 3. Correlations between parameters

Correlated Parameters	Correlation Coefficient (r)
TEWL versus SCORAD	0.560**
TEWL versus SAXD peak II position	0.450**
TEWL versus FTIR scissoring bandwidth	−0.735**
TEWL versus FTIR stretching	0.645**
TEWL versus total C34 CER content	0.738**
TEWL versus total CER [EO] content	−0.441**
TEWL versus average CER chain length	−0.528**
TEWL versus NMF	−0.643**
SCORAD versus SAXD peak II position	0.164
SCORAD versus FTIR scissoring bandwidth	−0.474*
SCORAD versus FTIR stretching	0.534**
SCORAD versus total C34 CER content	−0.470*
SCORAD versus total CER [EO] content	−0.238
SCORAD versus average CER chain length	−0.265
SCORAD versus NMF	−0.362*
NMF versus SAXD peak II position	−0.501**
NMF versus FTIR scissoring bandwidth	0.697**
NMF versus FTIR stretching	−0.778**
NMF versus total C34 CER content	−0.611**
NMF versus total CER [EO] content	0.416**
NMF versus average CER chain length	0.456**

The SCORAD indicates the severity of AE and gives valid values only when AE is diagnosed. Therefore, all control subjects were excluded in these specific correlations.
*Correlation is significant at the 0.05 level.
**Correlation is significant at the 0.01 level.

In addition, the results show changed levels in some of the CER subclasses consistent with previous reports: a decrease in CER [NP] level and an increase in CER [AS] level (12, 34–37, 54, 55). We did not observe a change in CER/protein levels between AE patients and controls. Interestingly, the reduction in CER chain length found in the present study had a much stronger impact on the skin barrier function than did the changes in CER subclass levels: the TEWL increases proportionally with decreasing chain length. These findings are in excellent agreement with earlier in vitro studies showing that a reduction in chain length of CERs has a stronger impact on the lipid organization and permeability than a change in the ratio between CER subclasses keeping the chain length approximately equal (Refs 56–58; M. Oguri, G. S. Gooris, and J. A. Bouwstra, unpublished data).

Di Nardo et al. observed a reduction in CER/CHOL ratio in nonlesional skin of AE patients, whereas other studies do not report a decrease in CER content in nonlesional AE skin (20, 35–37, 54). Groen et al. (58) observed that increasing the CER or FFA level while keeping the level of the other two main lipid classes equal did not affect the permeability in vitro. These studies suggest that the CER composition and chain length rather than the ratio between lipid classes play a major role in the increased TEWL in nonlesional skin in patients with AE. The increment in C34 CERs and decrement in CER [EO] suggest that elongation of the acyl chains is reduced. As the elongase family plays an important role in the elongation of fatty acids in the viable epidermis, we hypothesize that the higher abundance of C34 CERs may be due to a misbalance in the activity of some of the members of the elongase family (59, 60).

Several publications report on the lipid organization in AE patients: Pilgram et al. reported changes in lateral packing when comparing three AE patients with three controls (32). In a very recent study, we reported the first results on a very limited number of subjects, focusing on the lamellar phases and ceramide subclasses without examining the CER chain lengths (61). In addition, several studies focused on the (delayed or incomplete) lamellar body extrusion process in AE (62–64), possibly caused by reduced peroxisome proliferator-activated receptor activation (65). In the present study, we were particularly interested in the influence of CER chain length on the lipid organization in AE patients.

With respect to the lamellar lipid organization, we observed a shift in peak II position of the SAXD curves of SC of AE patients. This observation indicates a reduced value of the repeat distances of the lamellar phases and/or a reduced formation of the LPP (28). The correlation between SAXD peak II position with CER [EO] and C34 CER levels indicates that changes in these CER levels affect the lamellar organization. When focusing on the lateral organization, AE patients show a less dense lipid packing compared with controls that correlates strongly with a higher level of C34 CERs. This finding shows that CER chain length is also an important determinant of the lateral lipid organization in SC. The observed changes in lamellar and

lateral organization correlate with the increased TEWL levels and thus with an abnormal skin barrier function in patients with AE. The findings in this study strongly support the hypothesis that, in AE patients, a reduction in CER chain length leads to a change in lipid organization, which in turn leads to an impaired barrier function. In addition, the present study shows that this impaired barrier function is correlated with disease severity as determined by SCORAD, which is supported by literature (66, 67). This may indicate that, as a result of inflammation, lipid synthesis is influenced (even at nonlesional sites), and subsequently, the barrier function is decreased.

As *FLG* mutations are known to be predisposing factors for AE (17), an interesting question is whether lipid changes are associated with the presence of *FLG* mutations. We screened our subjects for four of the most prevalent *FLG* mutations accounting for 93% of the European *FLG* mutation spectrum (38). In our study cohort, there is no evidence that *FLG* mutations have an effect on CER composition and lipid organization. In contrast, in a recent study in ichtyosis vulgaris patients (68), changes in the lamellar organization were observed between the patients and controls. In that investigation, however, the majority of the patients were homozygote or compound heterozygote with respect to *FLG* mutations, and no inflammation was observed in these patients.

In previous studies, as well as in the current study, AE patients with *FLG* mutations showed significantly reduced NMF levels (22, 69). Remarkably, in this study, changes in lipids correlated with NMF levels but not with the presence or absence of *FLG* mutations. This suggests that between *FLG* gene (genotype) and NMF (phenotype), other (translational and environmental) factors may also influence NMF levels. These factors may include *FLG* copy numbers (repeat alleles on the *FLG* gene) (70) and interleukin levels, which can downregulate filaggrin expression (71). Changes in NMF levels are suggested to lead to a change in pH, and together with altered interleukin levels and protease activity, this may affect enzymes involved in CER biosynthesis (5, 68, 72–74) and, therefore, change the CER composition and lipid organization. Thus, despite the fact that we did not find a correlation between the lipids and *FLG* mutation status, filaggrin might play an indirect role in the decreased barrier function of AE patients, although the underlying mechanism remains unclear. Besides, other barrier proteins may be involved. This will be subject of future studies by our group.

In conclusion, in this study, we have shown that the CER chain length is altered in AE patients by elevated C34 CER levels and reduced CER [EO] levels. These changes correlate with an altered lipid organization and a decreased barrier function in AE patients. In addition, a significant correlation was observed between disease severity and change in lipid composition and organization. Our results suggest a novel therapeutic entry to repair skin barrier defects in AE patients, aimed at normalizing CER chain length distribution. Such a treatment could improve the SC lipid organization and restore the skin barrier function of AE patients.

The authors thank Cosmoferm for provision of the synthetic CER and the Netherlands Organization for Scientific Research (NWO) for provision of beam time.

REFERENCES

1. Proksch, E., R. Folster-Holst, and J. M. Jensen. 2006. Skin barrier function, epidermal proliferation and differentiation in eczema. *J. Dermatol. Sci.* **43:** 159–169.
2. Elias, P. M., and G. K. Menon. 1991. Structural and lipid biochemical correlates of the epidermal permeability barrier. *Adv. Lipid Res.* **24:** 1–26.
3. Masukawa, Y., H. Narita, H. Sato, A. Naoe, N. Kondo, Y. Sugai, T. Oba, R. Homma, J. Ishikawa, Y. Takagi, et al. 2009. Comprehensive quantification of ceramide species in human stratum corneum. *J. Lipid Res.* **50:** 1708–1719.
4. van Smeden, J., L. Hoppel, R. van der Heijden, T. Hankemeier, R. J. Vreeken, and J. A. Bouwstra. 2011. LC/MS analysis of stratum corneum lipids: ceramide profiling and discovery. *J. Lipid Res.* **52:** 1211–1221.
5. Cork, M. J., D. A. Robinson, Y. Vasilopoulos, A. Ferguson, M. Moustafa, A. MacGowan, G. W. Duff, S. J. Ward, and R. Tazi-Ahnini. 2006. New perspectives on epidermal barrier dysfunction in atopic dermatitis: gene-environment interactions. *J. Allergy Clin. Immunol.* **118:** 3–21; quiz 22–23.
6. Leung, D. Y., and T. Bieber. 2003. Atopic dermatitis. *Lancet.* **361:** 151–160.
7. Alanne, S., M. Nermes, R. Soderlund, and K. Laitinen. 2011. Quality of life in infants with atopic dermatitis and healthy infants: a follow-up from birth to 24 months. *Acta Paediatr.* **100:** e65–e70.
8. Mozaffari, H., Z. Pourpak, S. Pourseyed, A. Farhoodi, A. Aghamohammadi, M. Movahadi, M. Gharaghozloo, and M. Moin. 2007. Quality of life in atopic dermatitis patients. *J. Microbiol. Immunol. Infect.* **40:** 260–264.
9. Slattery, M. J., M. J. Essex, E. M. Paletz, E. R. Vanness, M. Infante, G. M. Rogers, and J. E. Gern. 2011. Depression, anxiety, and dermatologic quality of life in adolescents with atopic dermatitis. *J. Allergy Clin. Immunol.* **128:** 668–671.
10. van Valburg, R. W., M. G. Willemsen, P. C. Dirven-Meijer, A. P. Oranje, J. C. van der Wouden, and H. Moed. 2011. Quality of life measurement and its relationship to disease severity in children with atopic dermatitis in general practice. *Acta Derm. Venereol.* **91:** 147–151.
11. Williams, H., and C. Flohr. 2006. How epidemiology has challenged 3 prevailing concepts about atopic dermatitis. *J. Allergy Clin. Immunol.* **118:** 209–213.
12. Di Nardo, A., P. Wertz, A. Giannetti, and S. Seidenari. 1998. Ceramide and cholesterol composition of the skin of patients with atopic dermatitis. *Acta Derm. Venereol.* **78:** 27–30.
13. Yoshiike, T., Y. Aikawa, J. Sindhvananda, H. Suto, K. Nishimura, T. Kawamoto, and H. Ogawa. 1993. Skin barrier defect in atopic dermatitis: increased permeability of the stratum corneum using dimethyl sulfoxide and theophylline. *J. Dermatol. Sci.* **5:** 92–96.
14. Werner, Y., and M. Lindberg. 1985. Transepidermal water loss in dry and clinically normal skin in patients with atopic dermatitis. *Acta Derm. Venereol.* **65:** 102–105.
15. Seidenari, S., and G. Giusti. 1995. Objective assessment of the skin of children affected by atopic dermatitis: a study of pH, capacitance and TEWL in eczematous and clinically uninvolved skin. *Acta Derm. Venereol.* **75:** 429–433.
16. Elias, P. M., and M. Schmuth. 2009. Abnormal skin barrier in the etiopathogenesis of atopic dermatitis. *Curr. Opin. Allergy Clin. Immunol.* **9:** 437–446.
17. Palmer, C. N., A. D. Irvine, A. Terron-Kwiatkowski, Y. Zhao, H. Liao, S. P. Lee, D. R. Goudie, A. Sandilands, L. E. Campbell, F. J. Smith, et al. 2006. Common loss-of-function variants of the epidermal barrier protein filaggrin are a major predisposing factor for atopic dermatitis. *Nat. Genet.* **38:** 441–446.
18. Hudson, T. J. 2006. Skin barrier function and allergic risk. *Nat. Genet.* **38:** 399–400.
19. Seguchi, T., C. Y. Cui, S. Kusuda, M. Takahashi, K. Aisu, and T. Tezuka. 1996. Decreased expression of filaggrin in atopic skin. *Arch. Dermatol. Res.* **288:** 442–446.

20. Angelova-Fischer, I., A. C. Mannheimer, A. Hinder, A. Ruether, A. Franke, R. H. Neubert, T. W. Fischer, and D. Zillikens. 2011. Distinct barrier integrity phenotypes in filaggrin-related atopic eczema following sequential tape stripping and lipid profiling. *Exp. Dermatol.* **20:** 351–356.
21. Jakasa, I., E. S. Koster, F. Calkoen, W. H. McLean, L. E. Campbell, J. D. Bos, M. M. Verberk, and S. Kezic. 2011. Skin barrier function in healthy subjects and patients with atopic dermatitis in relation to filaggrin loss-of-function mutations. *J. Invest. Dermatol.* **131:** 540–542.
22. O'Regan, G. M., P. M. Kemperman, A. Sandilands, H. Chen, L. E. Campbell, K. Kroboth, R. Watson, M. Rowland, G. J. Puppels, W. H. McLean, et al. 2010. Raman profiles of the stratum corneum define 3 filaggrin genotype-determined atopic dermatitis endophenotypes. *J. Allergy Clin. Immunol.* **126:** 574–580.e1.
23. Jungersted, J. M., H. Scheer, M. Mempel, H. Baurecht, L. Cifuentes, J. K. Hogh, L. I. Hellgren, G. B. Jemec, T. Agner, and S. Weidinger. 2010. Stratum corneum lipids, skin barrier function and filaggrin mutations in patients with atopic eczema. *Allergy.* **65:** 911–918.
24. Flohr, C., K. England, S. Radulovic, W. H. McLean, L. E. Campbel, J. Barker, M. Perkin, and G. Lack. 2010. Filaggrin loss-of-function mutations are associated with early-onset eczema, eczema severity and transepidermal water loss at 3 months of age. *Br. J. Dermatol.* **163:** 1333–1336.
25. Winge, M. C., T. Hoppe, B. Berne, A. Vahlquist, M. Nordenskjold, M. Bradley, and H. Torma. 2011. Filaggrin genotype determines functional and molecular alterations in skin of patients with atopic dermatitis and ichthyosis vulgaris. *PLoS ONE.* **6:** e28254.
26. Elias, P. M. 2005. Stratum corneum defensive functions: an integrated view. *J. Invest. Dermatol.* **125:** 183–200.
27. Elias, P. M., and M. Steinhoff. 2008. "Outside-to-inside" (and now back to "outside") pathogenic mechanisms in atopic dermatitis. *J. Invest. Dermatol.* **128:** 1067–1070.
28. Bouwstra, J. A., G. S. Gooris, J. A. van der Spek, and W. Bras. 1991. Structural investigations of human stratum corneum by small-angle X-ray scattering. *J. Invest. Dermatol.* **97:** 1005–1012.
29. Madison, K. C., D. C. Swartzendruber, P. W. Wertz, and D. T. Downing. 1987. Presence of intact intercellular lipid lamellae in the upper layers of the stratum corneum. *J. Invest. Dermatol.* **88:** 714–718.
30. Ongpipattanakul, B., M. L. Francoeur, and R. O. Potts. 1994. Polymorphism in stratum corneum lipids. *Biochim. Biophys. Acta.* **1190:** 115–122.
31. Bommannan, D., R. O. Potts, and R. H. Guy. 1990. Examination of stratum corneum barrier function in vivo by infrared spectroscopy. *J. Invest. Dermatol.* **95:** 403–408.
32. Pilgram, G. S., D. C. Vissers, H. van der Meulen, S. Pavel, S. P. Lavrijsen, J. A. Bouwstra, and H. K. Koerten. 2001. Aberrant lipid organization in stratum corneum of patients with atopic dermatitis and lamellar ichthyosis. *J. Invest. Dermatol.* **117:** 710–717.
33. Bouwstra, J. A., and M. Ponec. 2006. The skin barrier in healthy and diseased state. *Biochim. Biophys. Acta.* **1758:** 2080–2095.
34. Bleck, O., D. Abeck, J. Ring, U. Hoppe, J. P. Vietzke, R. Wolber, O. Brandt, and V. Schreiner. 1999. Two ceramide subfractions detectable in Cer(AS) position by HPTLC in skin surface lipids of non-lesional skin of atopic eczema. *J. Invest. Dermatol.* **113:** 894–900.
35. Farwanah, H., K. Raith, R. H. Neubert, and J. Wohlrab. 2005. Ceramide profiles of the uninvolved skin in atopic dermatitis and psoriasis are comparable to those of healthy skin. *Arch. Dermatol. Res.* **296:** 514–521.
36. Imokawa, G., A. Abe, K. Jin, Y. Higaki, M. Kawashima, and A. Hidano. 1991. Decreased level of ceramides in stratum corneum of atopic dermatitis: an etiologic factor in atopic dry skin? *J. Invest. Dermatol.* **96:** 523–526.
37. Ishikawa, J., H. Narita, N. Kondo, M. Hotta, Y. Takagi, Y. Masukawa, T. Kitahara, Y. Takema, S. Koyano, S. Yamazaki, et al. 2010. Changes in the ceramide profile of atopic dermatitis patients. *J. Invest. Dermatol.* **130:** 2511–2514.
38. Chen, H., J. E. Common, R. L. Haines, A. Balakrishnan, S. J. Brown, C. S. Goh, H. J. Cordell, A. Sandilands, L. E. Campbell, K. Kroboth, et al. 2011. Wide spectrum of filaggrin-null mutations in atopic dermatitis highlights differences between Singaporean Chinese and European populations. *Br. J. Dermatol.* **165:** 106–114.
39. Sandilands, A., A. Terron-Kwiatkowski, P. R. Hull, G. M. O'Regan, T. H. Clayton, R. M. Watson, T. Carrick, A. T. Evans, H. Liao, Y. Zhao, et al. 2007. Comprehensive analysis of the gene encoding filaggrin uncovers prevalent and rare mutations in ichthyosis vulgaris and atopic eczema. *Nat. Genet.* **39:** 650–654.
40. [No author] 1993. Severity scoring of atopic dermatitis: the SCORAD index. Consensus Report of the European Task Force on Atopic Dermatitis. *Dermatology.* **186:** 23–31.
41. Caspers, P. J., G. W. Lucassen, E. A. Carter, H. A. Bruining, and G. J. Puppels. 2001. In vivo confocal Raman microspectroscopy of the skin: noninvasive determination of molecular concentration profiles. *J. Invest. Dermatol.* **116:** 434–442.
42. Caspers, P. J., G. W. Lucassen, and G. J. Puppels. 2003. Combined in vivo confocal Raman spectroscopy and confocal microscopy of human skin. *Biophys. J.* **85:** 572–580.
43. Kalia, Y. N., I. Alberti, A. Naik, and R. H. Guy. 2001. Assessment of topical bioavailability in vivo: the importance of stratum corneum thickness. *Skin Pharmacol. Appl. Skin Physiol.* **14(Suppl. 1):** 82–86.
44. Voegeli, R., J. Heiland, S. Doppler, A. V. Rawlings, and T. Schreier. 2007. Efficient and simple quantification of stratum corneum proteins on tape strippings by infrared densitometry. *Skin Res. Technol.* **13:** 242–251.
45. Bligh, E. G., and W. J. Dyer. 1959. A rapid method of total lipid extraction and purification. *Can. J. Biochem. Physiol.* **37:** 911–917.
46. Thakoersing, V. S., M. Ponec, and J. A. Bouwstra. 2010. Generation of human skin equivalents under submerged conditions-mimicking the in utero environment. *Tissue Eng. Part A.* **16:** 1433–1441.
47. Motta, S., M. Monti, S. Sesana, R. Caputo, S. Carelli, and R. Ghidoni. 1993. Ceramide composition of the psoriatic scale. *Biochim. Biophys. Acta.* **1182:** 147–151.
48. Boncheva, M., F. Damien, and V. Normand. 2008. Molecular organization of the lipid matrix in intact Stratum corneum using ATR-FTIR spectroscopy. *Biochim. Biophys. Acta.* **1778:** 1344–1355.
49. Damien, F., and M. Boncheva. 2010. The extent of orthorhombic lipid phases in the stratum corneum determines the barrier efficiency of human skin in vivo. *J. Invest. Dermatol.* **130:** 611–614.
50. Tanojo, H., A. Bos-van Geest, J. A. Bouwstra, H. E. Junginger, and H. E. Bodde. 1997. In vitro human skin barrier perturbation by oleic acid: thermal analysis and freeze fracture electron microscopy studies. *Thermochim. Acta.* **293:** 77–85.
51. Schreiner, V., G. S. Gooris, S. Pfeiffer, G. Lanzendorfer, H. Wenck, W. Diembeck, E. Proksch, and J. Bouwstra. 2000. Barrier characteristics of different human skin types investigated with X-ray diffraction, lipid analysis, and electron microscopy imaging. *J. Invest. Dermatol.* **114:** 654–660.
52. Bras, W., I. P. Dolbnya, D. Detollenaere, R. van Tol, M. Malfois, G. N. Greaves, A. J. Ryan, and E. Heeley. 2003. Recent experiments on a combined small-angle/wide-angle X-ray scattering beam line at the ESRF. *J. Appl. Cryst.* **36:** 791–794.
53. Moore, D. J., M. E. Rerek, and R. Mendelsohn. 1997. FTIR spectroscopy studies of the conformational order and phase behavior of ceramides. *J. Phys. Chem. B.* **101:** 8933–8940.
54. Yamamoto, A., S. Serizawa, M. Ito, and Y. Sato. 1991. Stratum corneum lipid abnormalities in atopic dermatitis. *Arch. Dermatol. Res.* **283:** 219–223.
55. Matsumoto, M., N. Umemoto, H. Sugiura, and M. Uehara. 1999. Difference in ceramide composition between "dry" and "normal" skin in patients with atopic dermatitis. *Acta Derm. Venereol.* **79:** 246–247.
56. de Jager, M., W. Groenink, R. Bielsa i Guivernau, E. Andersson, N. Angelova, M. Ponec, and J. Bouwstra. 2006. A novel in vitro percutaneous penetration model: evaluation of barrier properties with p-aminobenzoic acid and two of its derivatives. *Pharm. Res.* **23:** 951–960.
57. de Sousa Neto, D., G. Gooris, and J. Bouwstra. 2011. Effect of the omega-acylceramides on the lipid organization of stratum corneum model membranes evaluated by X-ray diffraction and FTIR studies (Part I). *Chem. Phys. Lipids.* **164:** 184–195.
58. Groen, D., D. S. Poole, G. S. Gooris, and J. A. Bouwstra. 2011. Is an orthorhombic lateral packing and a proper lamellar organization important for the skin barrier function? *Biochim. Biophys. Acta.* **1808:** 1529–1537.
59. Ohno, Y., S. Suto, M. Yamanaka, Y. Mizutani, S. Mitsutake, Y. Igarashi, T. Sassa, and A. Kihara. 2010. ELOVL1 production of C24 acyl-CoAs is linked to C24 sphingolipid synthesis. *Proc. Natl. Acad. Sci. USA.* **107:** 18439–18444.

60. Park, Y. H., W. H. Jang, J. A. Seo, M. Park, T. R. Lee, D. K. Kim, and K. M. Lim. 2012. Decrease of ceramides with very long-chain fatty acids and downregulation of elongases in a murine atopic dermatitis model. *J. Invest. Dermatol.* **132:** 476–479.
61. Janssens, M., J. van Smeden, G. S. Gooris, W. Bras, G. Portale, P. J. Caspers, R. J. Vreeken, S. Kezic, A. P. Lavrijsen, and J. A. Bouwstra. 2011. Lamellar lipid organization and ceramide composition in the stratum corneum of patients with atopic eczema. *J. Invest. Dermatol.* **131:** 2136–2138.
62. Fartasch, M., I. D. Bassukas, and T. L. Diepgen. 1992. Disturbed extruding mechanism of lamellar bodies in dry non-eczematous skin of atopics. *Br. J. Dermatol.* **127:** 221–227.
63. Marsella, R., D. Samuelson, and K. Doerr. 2010. Transmission electron microscopy studies in an experimental model of canine atopic dermatitis. *Vet. Dermatol.* **21:** 81–88.
64. Scharschmidt, T. C., M. Q. Man, Y. Hatano, D. Crumrine, R. Gunathilake, J. P. Sundberg, K. A. Silva, T. M. Mauro, M. Hupe, S. Cho, et al. 2009. Filaggrin deficiency confers a paracellular barrier abnormality that reduces inflammatory thresholds to irritants and haptens. *J. Allergy Clin. Immunol.* **124:** 496–506, 506.e1–6.
65. Man, M. Q., G. D. Barish, M. Schmuth, D. Crumrine, Y. Barak, S. Chang, Y. Jiang, R. M. Evans, P. M. Elias, and K. R. Feingold. 2008. Deficiency of PPARbeta/delta in the epidermis results in defective cutaneous permeability barrier homeostasis and increased inflammation. *J. Invest. Dermatol.* **128:** 370–377.
66. Chamlin, S. L., J. Kao, I. J. Frieden, M. Y. Sheu, A. J. Fowler, J. W. Fluhr, M. L. Williams, and P. M. Elias. 2002. Ceramide-dominant barrier repair lipids alleviate childhood atopic dermatitis: changes in barrier function provide a sensitive indicator of disease activity. *J. Am. Acad. Dermatol.* **47:** 198–208.
67. Nemoto-Hasebe, I., M. Akiyama, T. Nomura, A. Sandilands, W. H. McLean, and H. Shimizu. 2009. Clinical severity correlates with impaired barrier in filaggrin-related eczema. *J. Invest. Dermatol.* **129:** 682–689.
68. Gruber, R., P. M. Elias, D. Crumrine, T. K. Lin, J. M. Brandner, J. P. Hachem, R. B. Presland, P. Fleckman, A. R. Janecke, A. Sandilands, et al. 2011. Filaggrin genotype in ichthyosis vulgaris predicts abnormalities in epidermal structure and function. *Am. J. Pathol.* **178:** 2252–2263.
69. Kezic, S., P. M. Kemperman, E. S. Koster, C. M. de Jongh, H. B. Thio, L. E. Campbell, A. D. W. H. I. McLean, G. J. Puppels, and P. J. Caspers. 2008. Loss-of-function mutations in the filaggrin gene lead to reduced level of natural moisturizing factor in the stratum corneum. *J. Invest. Dermatol.* **128:** 2117–2119.
70. Irvine, A. D., W. H. I. McLean, and D. Y. M. Leung. 2011. Filaggrin mutations associated with skin and allergic diseases. *N. Engl. J. Med.* **365:** 1315–1327.
71. Howell, M. D., B. E. Kim, P. Gao, A. V. Grant, M. Boguniewicz, A. Debenedetto, L. Schneider, L. A. Beck, K. C. Barnes, and D. Y. Leung. 2007. Cytokine modulation of atopic dermatitis filaggrin skin expression. *J. Allergy Clin. Immunol.* **120:** 150–155.
72. Hachem, J. P., M. Q. Man, D. Crumrine, Y. Uchida, B. E. Brown, V. Rogiers, D. Roseeuw, K. R. Feingold, and P. M. Elias. 2005. Sustained serine proteases activity by prolonged increase in pH leads to degradation of lipid processing enzymes and profound alterations of barrier function and stratum corneum integrity. *J. Invest. Dermatol.* **125:** 510–520.
73. Nakagawa, N., S. Sakai, M. Matsumoto, K. Yamada, M. Nagano, T. Yuki, Y. Sumida, and H. Uchiwa. 2004. Relationship between NMF (lactate and potassium) content and the physical properties of the stratum corneum in healthy subjects. *J. Invest. Dermatol.* **122:** 755–763.
74. Schmid-Wendtner, M. H., and H. C. Korting. 2006. The pH of the skin surface and its impact on the barrier function. *Skin Pharmacol. Physiol.* **19:** 296–302.